

Live-cell imaging of alkyne-tagged small biomolecules by stimulated Raman scattering

Lu Wei¹, Fanghao Hu¹, Yihui Shen¹, Zhixing Chen¹, Yong Yu², Chih-Chun Lin², Meng C Wang² & Wei Min^{1,3}

Sensitive and specific visualization of small biomolecules in living systems is highly challenging. We report stimulated Raman-scattering imaging of alkyne tags as a general strategy for studying a broad spectrum of small biomolecules in live cells and animals. We demonstrate this technique by tracking alkyne-bearing drugs in mouse tissues and visualizing *de novo* synthesis of DNA, RNA, proteins, phospholipids and triglycerides through metabolic incorporation of alkyne-tagged small precursors.

Innovations in light microscopy, particularly fluorescence imaging, have tremendously expanded our knowledge at the microscopic level¹. Common fluorescent tags are relatively bulky, however—when used to tag small biomolecules, they often considerably alter biological activity. An alternative strategy is label-free imaging using intrinsic contrasts^{2–4}. However, label-free approaches such as Raman spectroscopy are often hindered by poor molecular selectivity. How to specifically and sensitively image small biomolecules thus remains highly challenging despite their importance in biomedicine.

Here we report an effective imaging modality for small biomolecules that uses stimulated Raman scattering (SRS) microscopy to image alkynes (that is, C≡C) as nonlinear vibrational tags (**Supplementary Fig. 1**). Alkynes possess desirable chemical and spectroscopic features. Chemically, they are small (only two atoms), exogenous (nearly non-existent inside cells) and bioorthogonal (inert to reactions with endogenous biomolecules). These properties render alkynes key players in bioorthogonal chemistry, in which precursors labeled with alkyne tags form covalent bonds with azides fused to probes such as fluorophores for detection^{5–12}. However, such a ‘click-chemistry’ approach prohibits live imaging, as it usually involves a copper-catalyzed reaction^{7–11} that requires cell fixation, and the copper-free version has slow kinetics and high background¹². Spectroscopically, the C≡C stretching motion shows a substantial change of polarizability,

displaying a sharp Raman peak around 2,125 cm⁻¹, which lies in a cell-silent spectral region¹³, where no other peaks exist (**Fig. 1a**). Compared to the popular carbon-deuterium (C-D) Raman tag¹⁴, alkynes produce peaks that are about 40 times higher. For this reason, alkynes have been used as tags by recent spontaneous-Raman studies^{15,16}; however, the signal is still relatively weak, and extremely long acquisition times (~49 min per frame consisting of 127 × 127 pixels) limit dynamic imaging in live systems.

The coupling of SRS microscopy to alkyne tags that we report offers sensitivity, specificity and biocompatibility for probing complex living systems. When the energy difference between incident photons from two lasers (pump and Stokes) matches with the 2,125-cm⁻¹ mode of alkyne vibrations, the joint action of the photons will greatly accelerate the vibrational excitation of alkyne bonds. As a result of energy exchange between the input photons and alkynes, the output pump and Stokes beams will experience intensity loss and gain, respectively. Such intensity changes measured by SRS microscopy generate concentration-dependent alkyne distributions in three dimensions (3D; **Supplementary Fig. 1**).

SRS microscopy offers a number of advantages. First, SRS boosts vibrational excitation by a factor of 10⁷, rendering a quantum leap of sensitivity (that is, detectability and speed)^{17,18} over spontaneous Raman³. Second, we use a 6-ps pulse width to match the excitation profile of alkyne (**Fig. 1a**), assuring efficient and selective nonlinear excitation. Third, SRS is free of background¹⁸, whereas spontaneous Raman suffers from autofluorescence, and coherent anti-Stokes Raman scattering (CARS) suffers from nonresonant background³. Additional advantages include the use of near-infrared laser wavelengths for enhanced tissue penetration, intrinsic 3D sectioning (due to nonlinear excitation) and minimal phototoxicity.

We first detected the alkyne-tagged thymidine analog 5-ethynyl-2'-deoxyuridine (EdU)⁷ in solution (**Fig. 1b**). Under a fast acquisition time of 100 μs, we determined its detection limit to be 200 μM, corresponding to 12,000 alkynes within the laser focus. This approaches the shot-noise limit ($\Delta I_p/I_p \approx 2 \times 10^{-7}$) of the pump beam, which represents the maximum theoretical sensitivity of the system. To explore the general applicability of our approach, we went on to examine a broad spectrum of small biomolecules including alkyne-tagged deoxyribonucleosides, ribonucleosides, amino acids, choline molecules and fatty acids (**Fig. 1c**), whose metabolic incorporation has been thoroughly tested in bioorthogonal chemistry studies^{7–11}.

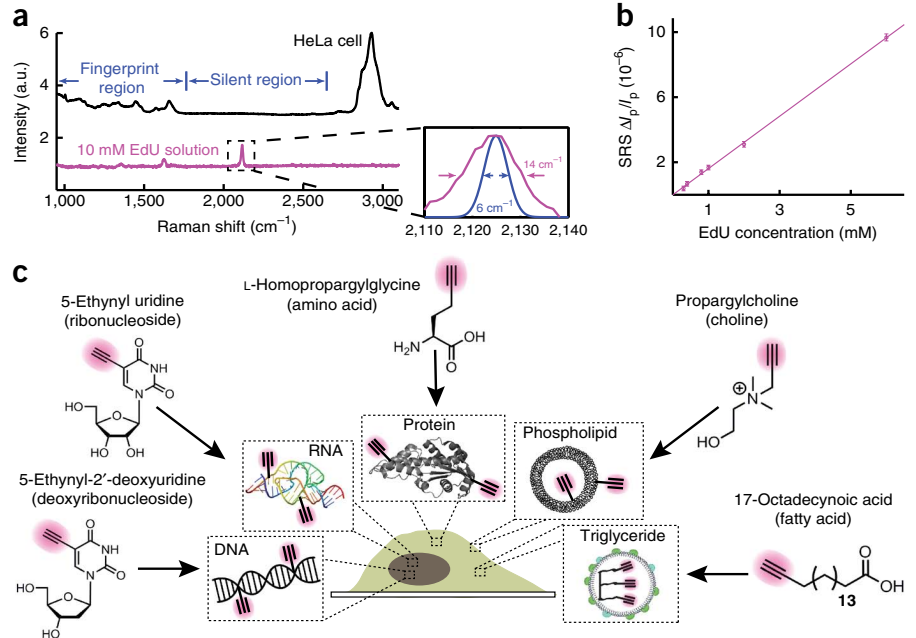
We imaged the metabolic uptake of EdU during *de novo* DNA synthesis. HeLa cells grown in medium with EdU show a sharp Raman peak at 2,125 cm⁻¹ in the cell-silent region (**Supplementary Fig. 2**). Live-cell SRS imaging revealed EdU

¹Department of Chemistry, Columbia University, New York, New York, USA. ²Department of Molecular and Human Genetics, Baylor College of Medicine, Houston, Texas, USA. ³Kavli Institute for Brain Science, Columbia University, New York, New York, USA. Correspondence should be addressed to W.M. (wm2256@columbia.edu).

RECEIVED 2 OCTOBER 2013; ACCEPTED 29 JANUARY 2014; PUBLISHED ONLINE 2 MARCH 2014; DOI:10.1038/NMETH.2878

Figure 1 | Bond-selective SRS imaging of alkynes as nonlinear vibrational tags.

(a) Spontaneous-Raman spectra of HeLa cells and 10 mM EdU solution. Inset shows the calculated SRS excitation profile (full-width at half-maximum (FWHM) = 6 cm^{-1} , blue), which is well fitted within the 2,125- cm^{-1} alkyne peak (FWHM = 14 cm^{-1} , magenta). (b) Linear dependence of stimulated Raman loss signals (2,125 cm^{-1}) with EdU concentrations under a 100- μs acquisition time. (c) The metabolic incorporation scheme for a broad spectrum of alkyne-tagged small precursors. a.u., arbitrary units.

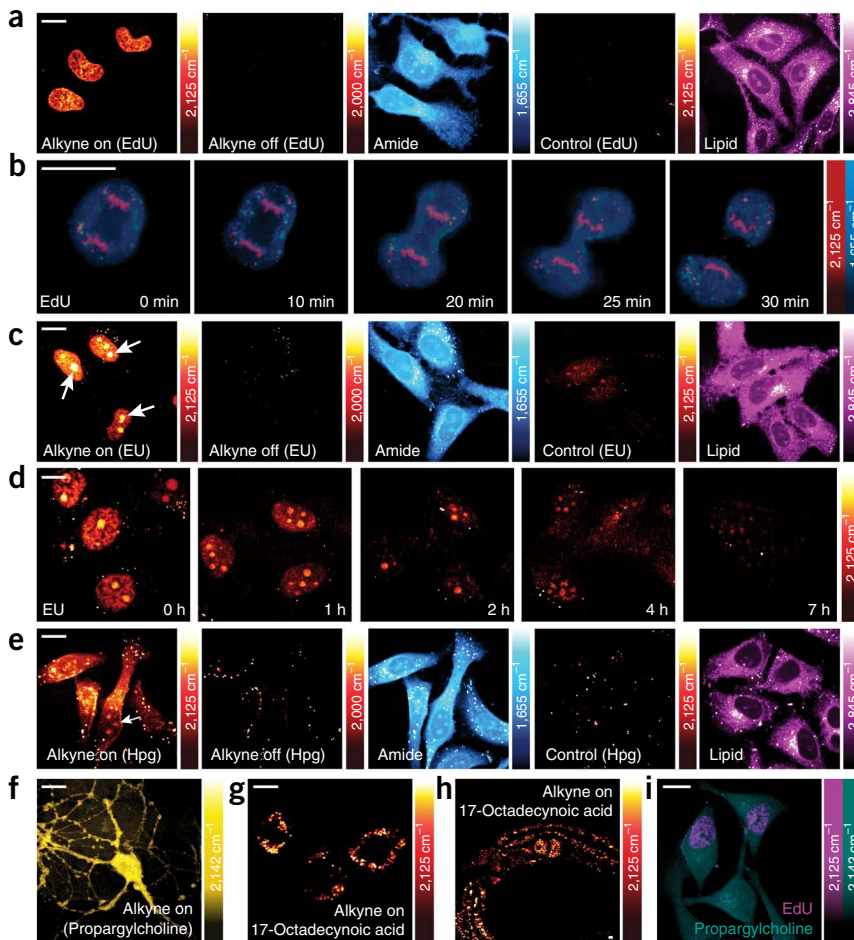


incorporation into the newly synthesized genomes of dividing cells (Fig. 2a, 'alkyne on'). Off-resonance images of the same cells, taken when the energy difference between pump and Stokes photons does not match vibrational peaks ('alkyne off'), were background free, thereby confirming the purely chemical contrast of SRS. No EdU signal showed up in cells treated with the DNA-synthesis inhibitor hydroxyurea, whereas results with lipids imaged at 2,845 cm^{-1} verified that these cells were normal on a morphological basis. Moreover, we tracked dividing cells every 5 min during mitosis (Fig. 2b), demonstrating acquisition speed and compatibility with live dynamics that are nearly impossible with spontaneous Raman^{15,16}. We also showed

that our method is applicable to multicellular organisms. Actively proliferating cells could be clearly distinguished in *Caenorhabditis elegans* grown in the presence of EdU (Supplementary Fig. 3).

Next, we studied RNA transcription and turnover using the alkyne-tagged uridine analog 5-ethynyl uridine (EU)⁸ in HeLa cells (Supplementary Fig. 2). The alkyne-on image (Fig. 2c) reveals localized EU inside the nucleus with higher abundance in the nucleoli, which are major compartments of rRNA-rich ribosomal assembly, and nearly disappears in the presence of the RNA-synthesis inhibitor actinomycin D.

Figure 2 | Live SRS imaging of *de novo* synthesis of DNA, RNA, proteomes, phospholipids and triglycerides by metabolic incorporation of alkyne-tagged small precursors. (a) Live HeLa cells incubated with 100 μM EdU alone (alkyne on) and with 10 mM hydroxyurea (control). (b) Time-lapse images of a dividing cell incubated with 100 μM EdU. (c) Live HeLa cells incubated with 2 mM EU alone (alkyne on) and with 200 nM actinomycin D (control). (d) Pulse-chase imaging of RNA turnover in HeLa cells incubated with 2 mM EU for 12 h followed by EU-free medium. (e) Live HeLa cells incubated with 2 mM Hpg alone (alkyne on) and with 2 mM methionine (control). (f) Live neurons incubated with 1 mM propargylcholine (alkyne on). (g) Live macrophages incubated with 400 μM 17-ODYA (alkyne on). (h) *C. elegans* fed with 17-ODYA (alkyne on). (i) Dual-color images of simultaneous EdU (2,125 cm^{-1} , magenta) and propargylcholine (2,142 cm^{-1} , green) incorporation. For a, c and e, alkyne-off and amide images show the same set of cells as the alkyne-on images; lipid images capture the same cells as control images. Scale bars, 10 μm . Representative images of 10–15 trials.



Turnover dynamics are further demonstrated by pulse-chase SRS imaging (Fig. 2d), which indicates a short nuclear RNA lifetime (~3 h) in live HeLa cells.

Many intricate biological processes, such as long-term memory, require protein synthesis in a spatiotemporal-dependent manner. We imaged L-homopropargylglycine (Hpg), an alkyne-tagged analog of methionine⁹, to visualize newly synthesized proteomes. HeLa cells grown in methionine-deficient medium supplemented with Hpg displayed an alkyne peak (Supplementary Fig. 2) about 20 times lower than that of 10 mM EdU solution (Fig. 1a). The corresponding alkyne-on image (Fig. 2e) shows the distribution of newly synthesized proteins with spatial enrichment in the nucleoli, which experience rapid protein exchange. Similar to EdU in solution, alkynes in mammalian cells showed a detection limit approaching 200 μM (with 100- μs pixel dwell time) on the basis of an average signal-to-noise ratio of 2 as we obtained in HeLa cells. The Hpg signal was well retained in fixed cells (Supplementary Fig. 4), indicating little contribution from freely diffusing Hpg. Furthermore, adding methionine, which has a 500-fold-faster incorporation rate, to compete with Hpg caused the signal to disappear⁹ (Fig. 2e). Note that we verified the spatial patterns of EdU, EU and Hpg incorporation in live cells by performing click chemistry on fixed cells (Supplementary Fig. 5).

Lipid metabolism is critical for many functions in healthy and diseased tissues, but few nonperturbative tags are available to monitor lipids in the cell. We thus monitored the metabolic incorporation of alkyne-tagged choline and fatty acids. Hippocampal neurons grown on propargylcholine presented a clear 2,142- cm^{-1} Raman peak (Supplementary Fig. 2). Such a frequency shift from 2,125 cm^{-1} is due to the positive charge on the nitrogen near the alkyne (Fig. 1c). As revealed by enzymatic assays (Supplementary Fig. 6), the alkyne-on signal (Fig. 2f) mainly originates from newly synthesized choline phospholipids at membranes¹⁰. To label fatty acids, we incubated 17-octadecynoic acid (17-ODYA) with THP-1 macrophages, which actively scavenge cholesterol and fatty acids¹⁹. The alkyne-on image (Fig. 2g) depicts the formation of numerous lipid droplets that indicates transformation into foam cells, a hallmark of early atherosclerosis. Multicellular organisms are also capable of taking up 17-ODYA for lipid imaging. Upon SRS imaging, newly taken-up fatty acids in *C. elegans* appeared mainly inside lipid droplets, known to exist largely in the form of triglycerides²⁰ (Fig. 2h). Such a fat-accumulation process could serve as a useful model for studying obesity and diabetes. We were also able to perform dual-color imaging of propargylcholine (2,142 cm^{-1}) and EdU (2,125 cm^{-1}) incorporation owing to the spectral sharpness and separation of their two alkyne peaks (Fig. 2i).

Finally, we tracked alkyne-bearing drug delivery (Supplementary Figs. 7 and 8) in animal tissues by taking advantage of the intrinsic 3D-sectioning property of SRS. Unlike bulky fluorophores, alkynes have little perturbation to pharmacokinetics and are common moieties in many pharmaceuticals. We chose terbinafine hydrochloride (TH), a US Food and Drug Administration (FDA)-approved alkyne-bearing antifungal skin drug, and imaged its drug delivery pathways inside mouse ear tissue to a depth of about 100 μm by targeting its internal alkyne at 2,230 cm^{-1} . TH images captured at various depths all show patterns that highly resemble lipid distributions but not protein distributions, suggesting that

TH penetrates into tissues through the lipid phase, consistent with its lipophilic nature. Our technique should be applicable to tracking other drugs after proper alkyne derivatization.

In conclusion, we report a general strategy to image small and biologically vital molecules in live cells by coupling SRS microscopy with alkyne vibrational tags. Other nonlinear Raman techniques such as CARS and its derivatives might also be able to detect alkynes, but with potentially greater technical complications^{3,17}. The major advantages of SRS lie in the superior sensitivity, specificity and compatibility with dynamics of live cells and animals. SRS imaging of alkynes may do for small biomolecules what fluorescence imaging of fluorophores has done for larger species.

METHODS

Methods and any associated references are available in the [online version of the paper](#).

Note: Any Supplementary Information and Source Data files are available in the [online version of the paper](#).

ACKNOWLEDGMENTS

We thank L. Zhang, L. Brus, V.W. Cornish, D. Peterka and R. Yuste for helpful discussions. We are grateful to Y. Shin and X. Gao for technical assistance. W.M. acknowledges support from Columbia University, a US National Institutes of Health Director's New Innovator Award, the US Army Research Office (W911NF-12-1-0594) and an Alfred P. Sloan Research Fellowship.

AUTHOR CONTRIBUTIONS

L.W., F.H., Y.S., Z.C., Y.Y., C.-C.L. and M.C.W. performed experiments and analyzed data. L.W. and W.M. conceived the concept, designed the experiments and wrote the paper.

COMPETING FINANCIAL INTERESTS

The authors declare competing financial interests: details are available in the [online version of the paper](#).

Reprints and permissions information is available online at <http://www.nature.com/reprints/index.html>.

- Zhang, J., Campbell, R.E., Ting, A.Y. & Tsien, R.Y. *Nat. Rev. Mol. Cell Biol.* **3**, 906–918 (2002).
- Sasic, S. & Ozaki, Y. *Raman, Infrared, and Near-infrared Chemical Imaging* (Wiley, 2011).
- Cheng, J.-X. & Xie, X.S. *Coherent Raman Scattering Microscopy* (CRC Press, 2012).
- Masters, B.R. & So, P.T.C. *Handbook of Biomedical Nonlinear Optical Microscopy* (Oxford University Press, 2008).
- Prescher, J.A. & Bertozzi, C.R. *Nat. Chem. Biol.* **1**, 13–21 (2005).
- Grammel, M. & Hang, H.C. *Nat. Chem. Biol.* **9**, 475–484 (2013).
- Salic, A. & Mitchison, T.J. *Proc. Natl. Acad. Sci. USA* **105**, 2415–2420 (2008).
- Jao, C.Y. & Salic, A. *Proc. Natl. Acad. Sci. USA* **105**, 15779–15784 (2008).
- Beatty, K.E. et al. *Angew. Chem. Int. Ed.* **45**, 7364–7367 (2006).
- Jao, C.Y., Roth, M., Welti, R. & Salic, A. *Proc. Natl. Acad. Sci. USA* **106**, 15332–15337 (2009).
- Hang, H.C., Wilson, J.P. & Charron, G. *Acc. Chem. Res.* **44**, 699–708 (2011).
- Baskin, J.M. et al. *Proc. Natl. Acad. Sci. USA* **104**, 16793–16797 (2007).
- Lin-Vien, D., Colthup, N.B., Fateley, W.G. & Grasselli, J.G. *The Handbook of Infrared and Raman Characteristic Frequencies of Organic Molecules* 95–104 (Academic Press, 1991).
- Wei, L., Shen, Y., Yong, Y., Wang, M. & Min, W. *Proc. Natl. Acad. Sci. USA* **110**, 11226–11231 (2013).
- Yamakoshi, H. et al. *J. Am. Chem. Soc.* **133**, 6102–6105 (2011).
- Yamakoshi, H. et al. *J. Am. Chem. Soc.* **134**, 20681–20689 (2012).
- Min, W., Freudiger, C.W., Lu, S. & Xie, X.S. *Annu. Rev. Phys. Chem.* **62**, 507–530 (2011).
- Freudiger, C.W. et al. *Science* **322**, 1857–1861 (2008).
- Moore, K.J. & Tabas, I. *Cell* **145**, 341–355 (2011).
- Ashrafi, K. et al. *Nature* **421**, 268–272 (2003).

ONLINE METHODS

Bond-selective stimulated Raman scattering (SRS) microscopy.

See **Supplementary Figure 1** for details of the microscopy setup. An integrated laser system (picoEMERALD, Applied Physics & Electronics, Inc.) was chosen as the light source for both pump and Stokes beams. Briefly, picoEMERALD provides an output pulse train at 1,064 nm with 6-ps pulse width and 80-MHz repetition rate, which serves as the Stokes beam. The frequency doubled beam at 532 nm is used to synchronously seed a picosecond optical parametric oscillator (OPO) to produce a mode-locked pulse train with five~6 ps pulse width (the idler beam of the OPO is blocked with an interferometric filter). The output wavelength of the OPO is tunable from 720 to 990 nm, which serves as the pump beam. The intensity of the 1,064-nm Stokes beam is modulated sinusoidally by a built-in electro-optic modulator at 8 MHz with a modulation depth of more than 95%. The pump beam is then spatially overlapped with the Stokes beam by using a dichroic mirror inside picoEMERALD. The temporal overlap between pump and Stokes pulse trains is ensured with a built-in delay stage and optimized by the SRS signal of pure dodecane liquid at the microscope.

Pump and Stokes beams are coupled into an inverted multiphoton laser-scanning microscope (FV1200MPE, Olympus) optimized for near-IR throughput. A 60× water objective (UPlanAPO/IR, 1.2 N.A., Olympus) with high near-IR transmission is used for all cell imaging. The pump/Stokes beam size is matched to fill the back-aperture of the objective. The forward going pump and Stokes beams after passing through the sample are collected in transmission with a high N.A. condenser lens (oil immersion, 1.4 N.A., Olympus), which is aligned following Köhler illumination. A telescope is then used to image the scanning mirrors onto a large area (10 by 10 mm) Si photodiode (FDS1010, Thorlabs) to decan beam motion during laser scanning. The photodiode is reverse biased by 64 V from a DC power supply to increase both the saturation threshold and response bandwidth. A high O.D. bandpass filter (890/220 CARS, Chroma Technology) is placed in front of the photodiode to block the Stokes beam completely and to transmit the pump beam only.

The output current of the photodiode is electronically pre-filtered by an 8-MHz band-pass filter (KR 2724, KR Electronics) to suppress both the 80-MHz laser pulsing and the low-frequency fluctuations resulting from laser scanning across the scattering sample. It is then fed into a radio frequency lock-in amplifier (SR844, Stanford Research Systems) terminated with 50 Ω to demodulate the stimulated Raman loss signal experienced by the pump beam. The in-phase X-output of the lock-in amplifier is fed back into the analog interface box (FV10-ANALOG) of the microscope. The time constant is set for 10 μs (the shortest available with no additional filter applied). The current SRS imaging speed is limited by the shortest time constant available from the lock-in amplifier (SR844). For all imaging, 512 by 512 pixels are acquired for one frame with a 100 μs of pixel dwell time (26 s per frame) for laser scanning and 10 μs of time constant from the lock-in amplifier. Laser powers after 60× IR objective used for imaging are as follows: 130 mW for modulated Stokes beam; 120 mW for the pump beam in 2,133 cm⁻¹, 2,142 cm⁻¹, 2,000 cm⁻¹ and 1,655 cm⁻¹ channels, 85 mW for the pump beam in 2,230 cm⁻¹ and 2,300 cm⁻¹ channels, and 50 mW for the pump beam in 2,845 cm⁻¹ channels.

Spontaneous Raman spectroscopy. The spontaneous Raman spectra were acquired using a laser confocal Raman microscope (Xplora, Horiba Jobin Yvon) at room temperature. A 12 mW (after the microscope objective), 532-nm diode laser was used to excite the sample through a 50× air objective (MPlan N, 0.75 N.A., Olympus). The total data acquisition time was 300 s using the LabSpec 6 software. For all the spontaneous Raman spectra, we subtracted the PBS solution background.

Materials. 5-Ethynyl-2'-deoxyuridine (EdU) (T511285), 17-octadecynoic acid (17-ODYA) (O8382), DMEM medium without L-methionine, L-cysteine and L-glutamine (D0422), L-methionine (M5308), L-cysteine (C7602), 2-mercaptoethanol (M3148) and phorbol 12-myristate 13-acetate (P1585) were purchased from Sigma-Aldrich. 5-Ethynyl Uridine (EU) (E-10345), Homopropargylglycine (Hpg) (C10186), Alexa Fluor 488 Azide (A10266), Click-iT Cell Reaction Buffer Kit (C10269), DMEM medium (11965), FBS (10082), penicillin/streptomycin (15140), L-glutamine (25030), Neurobasal A Medium (10888) and B27 supplement (17504) were purchased from Invitrogen. RPMI-1640 medium (30-2001) was purchased from ATCC. BCS (hyclone SH30072) was purchased from Fisher Scientific.

DMEM culture medium was made by adding 10% (vol/vol) FBS and 1% (vol/vol) penicillin/streptomycin to the DMEM medium. Methionine-deficient culture medium was made by supplying 4 mM L-glutamine, 0.2 mM L-cystine, 10% FBS and 1% penicillin/streptomycin to the DMEM medium without L-methionine, L-cysteine and L-glutamine. RPMI-1640 culture medium was made of supplying the RPMI-1640 medium with 10% FBS, 1% penicillin/streptomycin and 50 μM 2-mercaptoethanol. Neuron culture medium was made of Neurobasal A Medium with 1× B27 supplement and 0.5 mM glutamine. Culture medium for NIH3T3 cells was made by adding 10% (vol/vol) BCS and 1% (vol/vol) penicillin/streptomycin to the DMEM medium.

Propargylcholine synthesis. Propargylcholine was synthesized as described previously¹⁰. 3 mL propargyl bromide (80 wt. % solution in toluene) were added dropwise to 3 g 2-dimethylaminoethanol in 10 mL anhydrous THF on ice under argon gas protection and stirring. The ice bath was removed and the mixture was kept stirring at room temperature overnight. The white solids were filtered the next day and washed extensively with cold anhydrous THF to obtain 5 g pure propargylcholine bromide. All chemicals here were purchased from Sigma-Aldrich. NMR spectrum was recorded on a Bruker 400 (400 MHz) Fourier Transform (FT) NMR spectrometer at the Columbia University Chemistry Department. ¹H NMR spectra are tabulated in the following order: multiplicity (s, singlet; d, doublet; t, triplet; m, multiplet), number of protons. ¹H NMR (400 MHz, D₂O) δ ppm: 4.37 (d, *J* = 2.4 Hz, 2H); 4.10 (m, 2H); 3.66 (t, *J* = 4.8 Hz, 2H); 3.28 (s, 6H); MS (APCI+) *m/z* Calcd. for C₇H₁₄NO [M]⁺: 128.19. Found: 128.26.

Sample preparation for SRS imaging of live cells and organisms. For all SRS imaging experiments of HeLa cells (**Fig. 2**), cells were first seeded on coverslips with a density of 1 × 10⁵/mL in petri dishes with 2 mL DMEM culture medium for 20 h at 37 °C and 5% CO₂.

For the EdU experiment, DMEM culture medium was then changed to DMEM medium (FBS-free) for 24 h for cell cycle

synchronization. After synchronization, medium was replaced back to DMEM culture medium and EdU (10 mM stock in PBS) was simultaneously added to a concentration of 100 μ M for 15 h.

For the EU experiment, EU (100 mM stock in PBS) was added to the DMEM culture medium directly to a concentration of 2 mM for 7 h.

For the Hpg experiment, DMEM culture medium was then changed to methionine-deficient culture medium for 1 h, followed by supplying 2 mM Hpg (200 mM stock in PBS) in the medium for 24 h.

For the propargylcholine and EdU dual-color experiment, DMEM culture medium was changed to DMEM medium (FBS-free) for synchronization. After synchronization, medium was replaced back to DMEM culture medium by simultaneously adding both propargylcholine (25 mM stock in PBS) and EdU (10 mM stock in PBS) to the culture medium to a concentration of 1 mM and 100 μ M, respectively, for 24 h.

For the propargylcholine experiment in neurons, hippocampal neurons were cultured on coverslips in 1 ml neuron culture medium for 14 d, and then propargylcholine (25 mM stock in PBS) is directly added into the medium to a final concentration of 1 mM for 24 h.

For the 17-ODYA experiment in macrophages, THP-1 cells were first seeded on coverslips at a density of 2×10^5 /mL in 2 ml RPMI-1640 culture medium for 24 h, followed by 72 h induction of differentiation to macrophages by incubating with 100 ng/ml Phorbol 12-myristate 13-acetate (PMA) in the medium. Medium was then replaced with RPMI-1640 culture medium containing 400 μ M 17-ODYA (6:1 complexed to BSA) for 15 h.

For all of the above experiments, after incubation, the coverslip is taken out to make an imaging chamber filled with PBS for SRS imaging.

For the 17-ODYA experiment in *C. elegans*, OP50 bacterial culture was mixed well with 4 mM 17-ODYA (from 100 mM ethanol stock solution), and then seeded onto nematode growth medium (NGM) plates. After drying the plates in a hood, wild-type N₂ day 1 adult *C. elegans* were placed onto the plates and fed for 40 h. *C. elegans* were then mounted on 2% agarose pads containing 0.1% NaN₃ as anesthetic on glass microscope slides for SRS imaging.

SRS imaging of *C. elegans* germline after feeding with EdU.

The MG1693 (thymidine-defective MG1655) *Escherichia coli* strain was cultured in 2 ml LB medium at 37 °C overnight, and transferred to 100 ml of M9 medium containing 400 μ M EdU for further growth at 37 °C for 24 h. The EdU-labeled MG1693 *E. coli* was then seeded on an M9 agar plate. Synchronized day 1 adult

worms developed in 20 °C were transferred to EdU-labeled bacterial plate for 3 h, and then were dissected to take out the germline for imaging (**Supplementary Fig. 3**).

Cell preparation for click chemistry–based fluorescence microscopy. All experiments (**Supplementary Fig. 5**) were carried out following the manufacturer's protocol from Invitrogen. HeLa cells were first incubated with 10 μ M EdU in DMEM culture medium for 24 h, or 1 mM EU in DMEM culture medium for 20 h or 1 mM Hpg in methionine-deficient culture medium for 20 h, respectively. Cells were then fixed in 4% PFA for 15 min, washed twice with 3% BSA in PBS and permeabilized with 0.5% Triton PBS solution for 20 min, followed by click-chemistry staining using Alexa Fluor 488 Azide in the Click-iT Cell Reaction Buffer Kit for 30 min. After washing with 3% BSA in PBS for three times, fluorescence images were obtained using an Olympus FV1200 confocal microscope with 488-nm laser excitation while the cells were immersed in PBS solution.

Enzymatic assays confirming propargylcholine incorporation into cellular choline phospholipids. We designed our control experiments according to the click chemistry–based assays previously reported¹⁰ (**Supplementary Fig. 6**). NIH 3T3 cells cultured with 0.5 mM propargylcholine for 48 h were fixed with 4% PFA for 15 min, rinsed with 1 mL TBS buffer twice and incubated with 1 mL 1 mg/mL BSA in TBS buffer for 1 h at 37 °C, with or without 0.02 U/mL phospholipase C (Type XIV from *Clostridium perfringens*, Sigma), in the presence of 10 mM CaCl₂ (required for phospholipase C activity) (**Supplementary Fig. 6b**) or 10 mM EDTA (**Supplementary Fig. 6c**). The cells were then washed with TBS buffer and ready for SRS imaging.

Sample preparation for drug delivery into mouse ear tissues.

Either DMSO solution or Drug cream (Lamisil, Novartis) containing 1% (w/w) active terbinafine hydrochloride (TH) was applied to the ears of an anesthetized live mouse (2–3 weeks old white mouse of either sex) for 30 min, and the dissected ears from the killed mouse were then imaged by SRS (**Supplementary Figs. 7 and 8**). 5 mice, 10 ears were used for the experiments. The amide (1,655 cm⁻¹) and lipid (2,845 cm⁻¹) images have been applied with linear spectral unmixing to eliminate cross talk before composition. The experimental protocol for drug delivery on mice (AC-AAAG4703) was approved by Institutional Animal Care and Use Committee at Columbia University.

Image progressing. Images are acquired with FluoView scanning software and assigned color or overlaid by ImageJ. Graphs were assembled with Adobe Illustrator.